Research Article

POSSIBLE PROTECTIVE ROLE OF NIGELLA SATIVA OIL ON CADMIUM INDUCED TOXICITY IN RAT RENAL CORTEX

Entesar A. Saber, Nashwa F. El-Tahawy, Seham A. Abdel Aleem, Azza H. Ali and Sara M. Naguib
Department of Histology,
El-Minia Faculty of Medicine

Abstract

Background: Cadmium (Cd) is one of the most toxic heavy metals. It is a serious environmental and occupational contaminant and represents a serious health hazard to human. **Aim of the study:** To describe the structural changes in rat renal cortex after $Cd(Cl)_{٢}$ administration and to shed a light on the possible protective effect of Nigella Sativa oil (NSO) against Cd- induced nephro-toxicity. **Materials and methods:** Twenty-one adult male albino rats were randomly divided into ٣ equal kg subcutaneously for ٢-/groups; group I; control: received isotonic NaCl in a daily dose of ٢ml kg subcutaneously for ٢-weeks. Group /weeks. Group II; received $Cd(Cl)_{٢}$ in a daily dose of ٠.٤٩ mg III was given NSO for ٣ days prior to and continued with the ٢-weeks of $Cd(Cl)_{٢}$ exposure, as a daily oral feeding of ٢ ml/kg. Animals were decapitated, kidneys were obtained and divided into two halves for separate processing; one for light microscopic and the other for transmission electron microscopic studies. The results were statistically analyzed. **Results:** There was a significant increase in plasma levels of urea and creatinine in group II, while administration of NSO in group III significantly decreased these levels. Various morphological changes and a significant increased $COX_{٢}$ expression in the renal cortex after $Cd(Cl)_{٢}$ exposure were observed. These morphological changes were in the form of peri-tubular capillary dilatation, interstitial hemorrhages, swollen renal glomeruli, glomerular & tubular cytoplasmic vacuolation, tubular distortion with dilated lumens, numerous vesicular mitochondria, and numerous lysosome. While administration of NSO, in group III, considerably ameliorate these changes and significantly decreased $COX_{٢}$ expression. **Conclusion:** Exposure of rats to $Cd(Cl)_{٢}$ induced Nephron-toxicity while administration of NSO ameliorate this toxic effect.

Key words: Nephro-toxicity, Cadmium chloride, Nigella sativa oil, Rats

Introduction

Cadmium (Cd) is one of the most toxic heavy metals, it is a serious environmental and occupational contaminant and may represent a serious health hazard to human and animals[١]. It is widely used in paints, plastic manufacturing, electrolysis, and industry[٢]. Moreover, tobacco contains significant amounts of Cd and smoking is one of the sources of Cd exposure in the general population[٣]. Atmospheric deposition of airborne Cd and the application of Cd-containing fertilizers and sewage sludge on farm land may lead to contamination of soils and increased Cd uptake by crops and vegetables consumed by human beings[٤]. The Cd absorption from the gastrointestinal tract is the main route of its

entry into human[٥]. It accumulates in various tissues after chronic exposure with food and water[٦]. It causes liver, kidney, and testis degeneration, hypertension, atherosclerosis, osteoporosis, anemia, and cancer[٧].

Herbal remedies are natural products derived from plants and plant extracts that have been traditionally used to treat various diseases or to promote general health[٨]. More attentions have been paid to the protective effects of natural anti-oxidants against chemicals-induced toxicities[٩]. Among the promising medicinal

plants is the Nigella sativa or black cumin that grows spontaneously and widely in several southern Mediterranean and Middle Eastern countries[١٠].

Thymoquinone is the bioactive and the most abundant constituent of Nigella Sativa oil (NSO) which has been shown to possess many therapeutic effects including; anti-inflammatory, anti-microbial, anti-cancer, anti-hypertensive, anti-diabetic, and anti-oxidants agent[١١].

Thymoquinone was found to be highly bioavailable providing significantly greater protection against free radical induced lipid peroxidation and DNA damage[١٢]. Thus many studies suggested that in-vivo and in-vitro thymoquinone exposure might protect multiple organs from a variety of toxic assaults[١٣].

The aim of this study was to describe the structural changes in the rat renal cortex after Cd(Cl)٢ administration and to shed a light on the possible protective effect of NSO against Cd- induced nephro-toxicity.

Material and Methods

Animals: Twenty-one adult (٢-٣ months), male albino rats (Sprague dawley strain) weighing ١٥٠-٢٠٠ g were used in this experiment in the Histology department of faculty of Medicine of El-Minia University. Rats were purchased from National Research Center, Cairo, Egypt. Every five rats were placed in a separate cage to avoid stress of isolation or overcrowding, and kept for ٥ days before experiment for acclimatization. They were allowed free access to tap water and standared rats' diet (El-Nile Company, Egypt). All experimental protocols were approved by the animal care committee of Minia University and coincide with international guidelines.

Reagents:

- Isotonic NaCl
- Cadmium chloride [Cd(Cl)٢] powder: was obtained from Sigma Aldrich (Egypt), which was freshly dissolved in isotonic NaCl according to manufacturer's instructions.
- Nigella Sativa oil (NSO): was purchased (pharco campany, Egypt) as soft gelatin capsules, each capsule containing ٤٥٠ mg of NOS.

Experimental design:

The rats were randomly divided into ٣ equal groups:

Group I (control group): consisted of ٧ rats received isotonic NaCl in a daily dose of ٢ml/kg subcutaneously for ٢-weeks.

Group II: consisted of ٧ rats were exposed to Cd(Cl)٢ in a daily dose of ٠.٤٩ mg/kg subcutaneously dissolved in ٢ ml isotonic NaCl for ٢-weeks[١٤].

Group III: consisted of ٧ rats received NSO for ٣ days prior to administration of Cd(Cl)٢ and continued with Cd(Cl)٢ for ٢- weeks, as a daily oral feeding of ٢ ml/kg[١٤].

At the end of experiment, all animals were sacrificed by decapitation under light halothane anesthesia.

Laboratory investigations:

For evaluation of renal function, blood samples were obtained via cardiac puncture with ٢ ١G needle mounted on ٥ ml syringe technique from all groups. Sera were separated and stored in aliquots at -٨٠°C till used for estimation of serum urea and creatinine[١٥].

Histological examinations:

Kidneys were rapidly removed and carefully dissected out for histological studies. After rinsing in normal saline, kidney tissues were divided into two halves for separate processing. One half processed for light microscopic study and the other half processed for transmission electron microscopic study.

Light Microscopic (LM) study:

For light microscopy, kidney specimens from all groups were fixed in ١٠٪ neutral-buffered formalin, dehydrated in a graded ethanol series, cleared in xylene embedded in paraffin wax, and sectioned into Six-micrometer sections.

- Some sections were stained with hemato-xylin and eosin (H&E)[١٦].
- Other sections were used for immune-histochemical staining for the COX٢ antibodies (inflammatory marker). Sections were de-paraffinized and rehydrated; to retrieve antigen, sections were incubated with ٠.١٪ trypsin and ٠.١٪ $CaCl_٢$ $٢H_٢O$ in Tris buffer (٥٠mmol/l) at pH ٧.٤ at ٣٧١C for ١٢٠ min. Sections were soaked in absolute methanol containing ٠.٣٪ hydrogen peroxide for ٣٠ min at room temperature, to eliminate endogenous pero-xidase activity. The sections were then incu-

bated with ١.٥٪ non-immunized goat serum for ٣٠ min at room temperature, then incubated with the diluted primary antibodies (١: ٥٠٠) for $COX_٢$ for ٣٠ min at room temperature, and washed three times with phosphate-buffered saline for ٣٠min. There-after, the sections were incubated with biotinylated goat antimouse immunoglobulin serum for ٦٠ min. After being washed with phosphate-buffered saline, the sections were incubated with avidin/biotin peroxidase complex (Vector, Burlingame, California, USA). Sites of peroxidase binding were detected using chromogenic ٣,٣٠-diamino-benzidine tetra hydrochloride substrate. Tissue sections were counterstained with hemato-xylin[١٧].

Image capture: Tissue sections were examined and images were digitally captured using a hardware consisting of a high-resolution color digital camera mounted on an Olympus microscope (Olympus, Japan), connected to a computer.

Ultra-structural study:
Kidney specimens were fixed in ٢.٥٪ phosphate buffered glutaraldehyde solution (pH ٧.٤) at ٤°C. After washing with phosphate buffer, the specimens were post-fixed for ١ h in ١٪ buffered osmium tetroxide solution. Subsequently, the specimens were dehydrated through an ascending series of ethanol, treated with propylene oxide and embedded in epoxy resin. After heat polymerization, ultrathin sections were cut using an ultramicrotome with a diamond knife and were double-stained with uranyl acetate and lead citrate to be examined and photographed by a TEM (JEOL, Japan) [١٨].

Morphometric study:
- The renal tissues were examined in random microscopic areas semi- quantitatively under ٤٠ high power fields, and the number of changes was assessed by counting of ٣ non overlapped fields for the same slide of each animal. The frequency and the severity of lesions in the kidneys were assessed semi-quantitatively [١٩] as: Score -: assigned normal, Score +: in between normal and mild, Score ++ (mild level): less than ٢٥٪ of the examined fields revealed histological alterations, Score +++ (moderate level): less than ٥٠٪ of the examined fields revealed histological alterations, and Score ++++ (severe level): less than ٧٥٪ of the total fields examined revealed histological alterations.
- The $COX_٢$ immunolabeled cells were counted. In each animal ٣ sections were examined, and cells were counted in ٣ adjacent non overlapping fields.

Data handling and statistics
Analysis of the laboratory findings and $COX_٢$ expression data were carried out using SPSS version ١٣ (SPSS Inc., Chicago, Illinois, USA). The following statistical tests were used: (١) Mean and standard deviation (MN ± SD) to describe quantitative data. (٢) Student's t-test was used to compare between two groups as regards parametric data. For all tests, a probability (P value) of less than ٠.٠٥ was considered significant.

Results

Laboratory findings
Serum levels of urea and creatinine of the control group showed normal levels. In the Cd-exposed group, there was significant increase in blood urea and creatinine levels compared to control while the results showed that the intake of NSO significantly decreased it (Table١).

Histological and immune-histochemical results:
A) H&E results:
Examination of the rat renal cortical tissue of control group showed normal architecture; numerous renal corpuscles (RC), proximal (PCTs) and distal (DCTs) convoluted tubules (Figs. ١,٢). The RC contained the glomeruli which surrounded by the Bowman's capsules with urinary spaces in between. The parietal layers were lined by simple squamous epithet-lium (Fig. ٣). The PCTs were lined with thick large cubical epithelium with acidophilic cytoplasm. The DCTs showed considerably lower cubical epithelium surrounding relatively larger regular distinct lumens. The macula densa cells (MDCs) were clearly observed as tall, narrow, and pale cells with central nuclei (Figs. ٢, ٣).

The histological changes in group II were variable and patchy; it showed peri-tubular capillary dilatations, interstitial hemorrhages, and inflammatory cell infiltration (Fig. ٤).

Marked enlargement of some vascular glomeruli which tightly filling the renal corpuscles with apparent obliteration of their Bowman's spaces were observed (Fig. ٥). Most renal corpuscular (Fig. ٥), PCT and DCT cells showed abundant cytoplasmic vaculations and tubular distortion (Fig. ٦).

Administration of NSO in group III ameliorated the damaging effects of $Cd(Cl)_2$. There were less peri-tubular capillary dilatations, interstitial hemorrhages, and inflammatory cell infiltration (Fig. ٧). Less tubular distortion (Fig. ٨), few glomeruli with narrow Bowman's spaces, and fewer cytoplasmic vaculations of the tubular cells were also observed (Fig. ٩).

Immuno-histochemical results:

The control group showed faint cytoplasmic expression in few MDCs, while cells of PCTs and DCTs displayed negative COX_2 immuno-reactivity (Fig. ١٠). In group II, most sections in this group displayed deeply stained COX_2 cytoplasmic expression in almost all MDCs, PCT and DCT cells (Figs. ١١). In group III, NSO seemed to decrease this cytoplasmic immune-reactivity in most MDCs, PCT and DCT cells if compared with group II (Fig. ١٢).

Statistically (Table ٢) showed that group II had a significant increase in COX_2 expression compared to the control group. Administration of NSO significantly decreased COX_2 expr-ession in group III compared to group II, but this decrease was still higher than the control as there was significant difference between this group and the control.

B)Transmission electron microscopic results:

In the control group, the endothelial cells of the glomerular capillaries were very richly fenestrated with large pores which lacked any closing diaphragm. Podocytes appeared adhering to endothelial walls and possessed short extensions in the form of many primary and secondary processes. The secondary processes were in contact with the basal lamina of the capillary walls. The regular filtration slits were clearly observed (Fig. ١٣)

The cells of PCTs were high cubical in shape and had central rounded nuclei with prominent nucleoli containing marginally arranged chromatin material. Their cell membranes were characterized by indistinct lateral borders, many long apical microvilli and basal infolding. Elongated mitochondria situated mainly between the nuclei and the uniformly thickened basement membrane (BMs). The cytoplasm showed also occasional lysosomes (Fig. ١٤).

The cells of DCTs were low cubical in shape and had central nuclei with prominent nucleoli. These cells were characterized by indistinct apical microvilli, clear cell boundary and basal infolding. Elongated mitochondria between the basal infolding were noticed (Fig. ١٥).

Group II showed marked morphological changes. Some renal glomerular endothelial cells showed loss of their fenestrae. Some pedicles became wide and appeared with dense matrix. Filtration slits were narrow in some areas while wide in other areas. Thickening of the glomerular basement membrane (GBM) was observed (Fig. ١٦). Both PCT cells (Fig. ١٧) and DCT cells (Fig. ١٨) showed nuclear chromatin condensation with loss of their nucleoli. The cytoplasm showed abnormal vesicular mito-chondria, more lysosomes and cytoplasmic vaculation. Thickening of the cellular BMs was also noticed. Irregular dense apical microvilli and loss of the basal infolding were noticed in the PCT cells.

In group III, administration of NSO decreased the morphological changes observed in group II. Few irregular fenestrae of the endothelial cells, few wide and dense pedicles were clearly observed. Less thickening of the BMs of glomerular blood capillaries was noticed (Fig. ١٩). The PCT cells (Fig. ٢٠) and DCT cells (Fig. ٢١) showed less nuclear chromatin condensation than in group IIa, but the nucleoli and basal infolding were still disappeared. The cytoplasm exhibited less lysosomes and cytoplasmic vaculation. The cellular BMs were less thickened if compared to group II. The apical microvilli of PCT cells were still irregular and dense.

Morphometric analysis:

The morphometric studies of $Cd(Cl)_2$ exposed group showed glomerular and tubular morphological changes at the light (Table ٣) and electron microscopic (Table ٤) levels.

These changes were suppressed by administration of NSO.

Table ١: Serum urea and creatinine levels in control and experimental groups (n=٧).

	Serum urea (mg/dL)				Serum creatinine (mg/dL)			
	MN ± SD	p-values			MN ± SD	p-value		
		P١	P٢	P٣		P١	P٢	P٣
١.Group I: control	٣١.٤ ± ٠.٦٧				٠.٤٤ ٠.٠٥			
٢.Group II:	٧٢.٥ ± ١.٠١	٠.٠٠٠*			٠.٨٩ ± ٠.٠٥	٠.٠٠١ *		
٣.Group III:	٣٤.٦ ± ٠.٧		٠.٠٠٠*	٠.٠٦١	٠.٥٢ ± ٠.٠٣		٠.٠٠١*	٠.٠٧١

*P < ٠.٠٥ is significant, P١: Cd group versus control; P٢: Cd+NSO group versus Cd group; P٣: Cd+NSO group versus control.

Table ٢: The $COX_{٢}$ expression in the control and the experimental groups (n=٧).

	MN ± SD	p-value		
		P١	P٢	P٣
Group I; Control group	٨ ± ٠.٣١٦			
Group II:	٢٢٩.٨ ± ٠.٨٦٠	٠.٠٠٠*		
Group III:	١٣٩.٨ ± ١.٣٩٣		٠.٠٠٠*	٠.٠٠٠*

*P < ٠.٠٥ is significant, P١: Cd group versus control; P٢: Cd+NSO group versus Cd group; P٣: Cd+NSO group versus control.

Table ٣: Scoring of morphological changes observed in the experimental groups by light microscope (n=٧):

Findings	Group I	Group II	Group III
Interstitial:			
-Hemorrhages and fibrosis	-	+++	++
-Inflammatory cells	-	+++	+
Renal corpuscles:			
-Glomerular vaculation	-	+++	++
-Enlarged renal corpuscles	-	++++	++
PCTs:			
-Tubular cells vaculation	-	+++	++
-Lumen widening and Distortion	-	+++	+
-Casts	-	-	-
DCTs			
-Tubular cells vaculation	-	+++	++
- Lumen widening and Distortion	-	+++	+
-Casts	-	-	-

Normal (-), in-between normal and mild (+), mild (++), moderate (+++) and sever (++++).

Table ٤: Scoring of morphological changes in control and experimental groups by Transmission Electron microscope (n=٧):

Findings	Group I	Group II	Group III
Renal glomeruli:			
- Irregular endothelial fenestra	-	+++/ lost	++
- BMs thickening	-	++++	++
- Narrowing of filtration slits	-	+++	++
- Fused pedicles	-	-	-
PCTs			
-Nuclear chromatin condensation	-	+++	++
-Disappearance of nucleoli	-	+++	+
-Apical brush border distortion	-	+++	++
-Absence of Basal infolding	-	++	+
-Numerous mitochondria	-	++++	+++
-Numerous lysosomes	-	++++	+++
DCTs			
-Nuclear chromatin condensation	-	+++	++
-Disappearance of nucleoli	-	+++	+
-Absence of Basal infolding	-	+++	++
-Numerous mitochondria	-	++++	+++
-Numerous lysosomes	-	++++	+++

Normal (-), in-between normal and mild (+), mild (++), moderate (+++) and sever (++++)

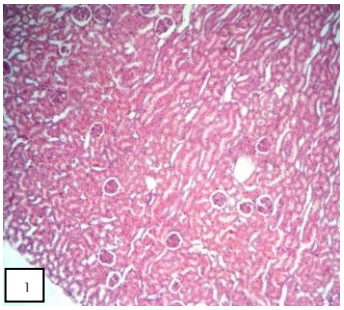

Fig. ١: A photomicrograph of renal cortex of group I showing normal lobular organization of the renal cortex. H&E X١٠٠

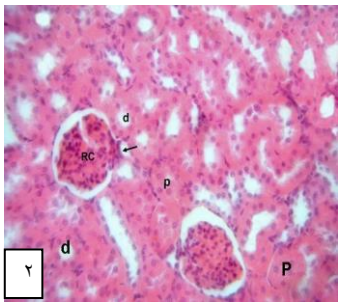

Fig.٢: A photomicrograph of renal cortex of group I showing the renal corpuscles (RC), PCTs (p) and DCTs (d). The convoluted tubules have a relatively regular distinct lumen. Notice the macula densa cells (arrow) of the DCT. H&E x٤٠٠

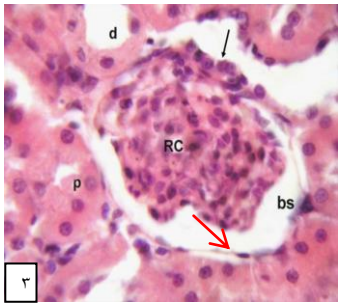

Fig.٣: A photomicrograph of renal cortex of group I showing a renal corpuscle (RC), parietal layer of Bowman's membrane (red arrow), and Bowman's space (bs). The PCTs (p) lined with thick cubical epithelium while DCTs (d) show lower cubical epithelium. Notice the macula densa cells (black arrow). H&E X١٠٠٠

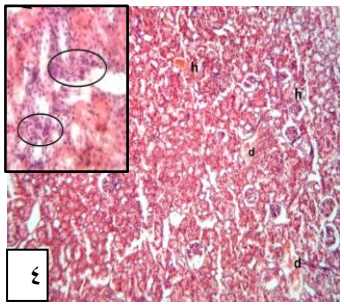

Fig.٤: A photomicrograph of renal cortex of group II showing architect-tural distortion, peri-tubular capillary dilatations (d), and interstitial hemorr-hages (h). The inset shows interstitial inflammatory cell infiltration (circles). H&E X١٠٠: inset x٤٠٠

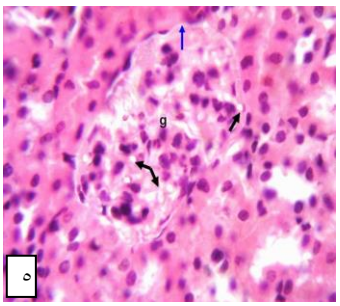

Fig.٥: A photomicrograph of renal cortex of group II showing markedly enlarged vascular glomerulus (g) with obliterated Bowman's space (blue arrow). Notice cytoplasmic vaculations (arrows) of corpuscular cells (black arrows). H&E X١٠٠٠

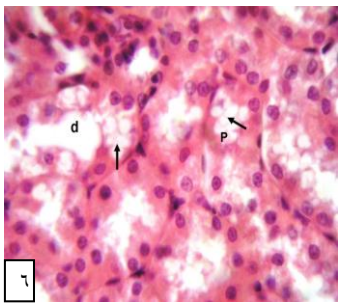

Fig. ٦: A photomicrograph of renal cortex of group II showing cytoplasmic vaculations (arrows) of the PCT (P) and DCT (d) cells. H&E X١٠٠٠

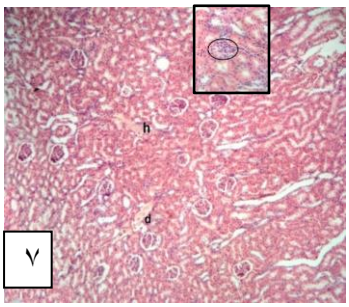

Fig.٧: A photomicrograph of renal cortex of group III showing less peri-tubular capillary dilatation (d) and hemorrhage (h) with preserved cortical architecture. Inset shows less obvious inflammatory cell invading the renal parenchyma (circle) than in group II.
H&E X١٠٠: inset x٤٠٠

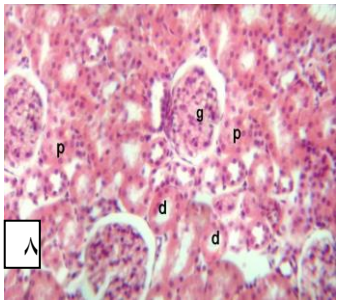

Fig.٨: A photomicrograph of renal cortex of group III showing less tubular distortion of PCTs (p) and DCTs (d) than in group II.
H&E X٤٠٠

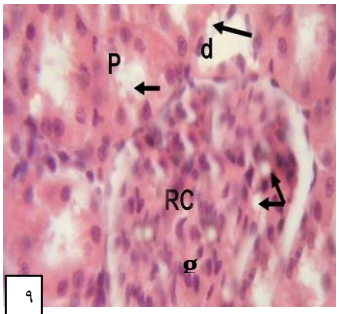

Fig.٩: A photomicrograph of renal cortex of group III showing less cytoplasmic vaculation (arrows) of the renal corpuscular cells (RC), PCT (P) and DCT cells (d) than in group II, with enlargement of the vascular glomeruli (g).
H&E X١٠٠٠

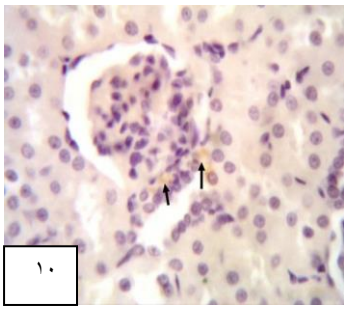

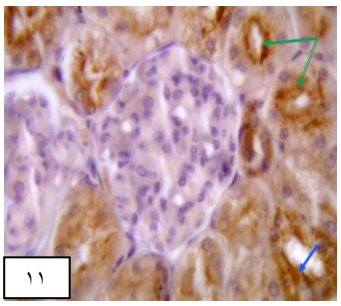

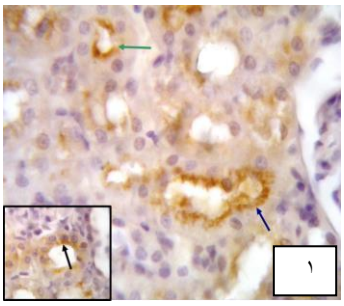

Photomicrographs of renal cortex labeled for COX٢ in:
Fig.١٠: group I showing faint COX٢ cytoplasmic expression in macula densa cells (arrows). Notice the negative immune-reactivity in the PCT and DCT cells.
Fig. ١١: group II showing deeply stained COX٢ cytoplasmic expression in most PCT (green arrows) and DCT (blue arrow) cells. Notice deeply stained COX٢ immuno-reactivity in the macula densa cells (black arrows).
Fig.١٢: group III showing less COX٢ cytoplasmic expression in PCT (green arrow), DCT (blue arrow) cells, and macula densa cells (inset, arrow) than in group II. Immuno-histochemistry counter stained with H x١٠٠٠

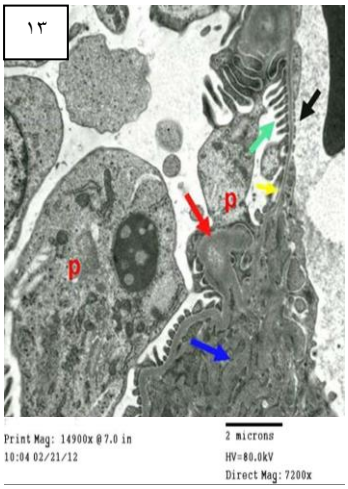

Fig.١٣: An electromicrograph of a renal glomerulus of group I showing a blood capillary with fenestrated endothelium (black arrow), ١ry (red arrow) and ٢ry process (blue arrow). Notice the filtration slits (green arrow) and the glomerular blood capillary BMs (yellow arrow). X٧٢٠٠

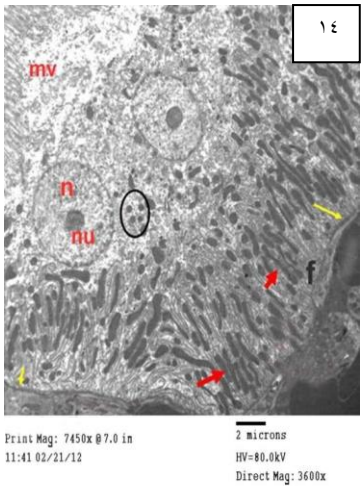

Fig.١٤: An electromicrograph of the PCT cells of group I showing rounded euchromatic nucleus (n) with prominent nucleolus (nu), apical microvilli (mv), basal infolding (f), elongated mitochondria (red arrows), lysosomes (circle) and the cellular BMs (yellow arrows). Notice indistinct lateral border. X٣٦٠٠

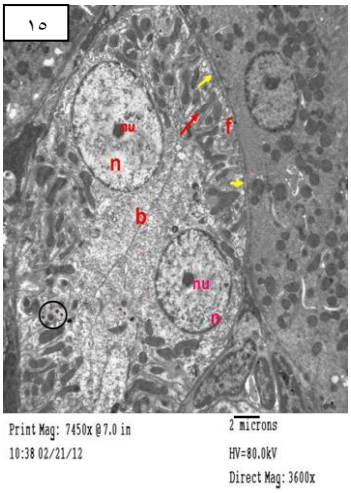

Fig.١٥: An electromicrograph of the DCT cells of group I showing rounded euchromatic nuclei (n) with prominent nucleoli (nu). Notice the indistinct apical microvilli, basal infolding (f) with basal mitochondria (red arrow), clear lateral border (b), lysosomes (circle) and the cellular BMs (yellow arrows). X٣٦٠٠

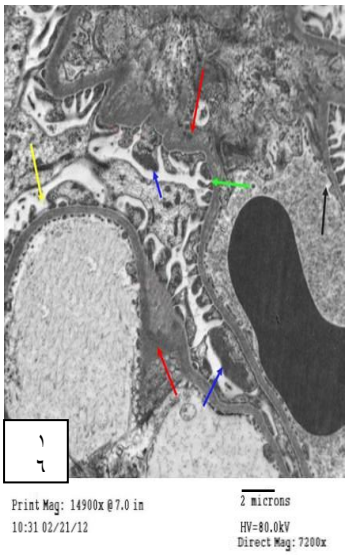

Fig.١٦: An electromicrograph of the renal glomerulus of group II showing blood capillaries with focal loss of their fenestrae (black arrow) and more wide dense pedicles (blue arrows). Notice the narrow (green arrow) and wide filtration slits (yellow arrow) in the same glomerulus and the thickened glomerular blood capillary BMs (red arrows). X٧٢٠٠

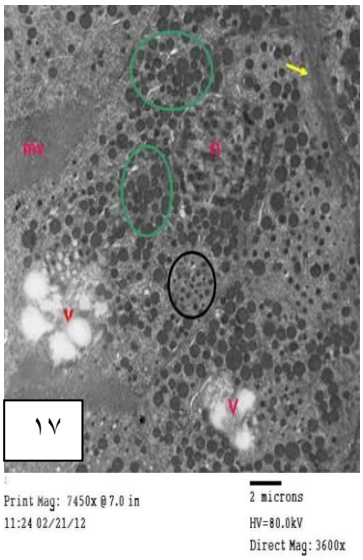

Fig.١٧: An electromicrograph of PCT cells of group II showing nuclear chromatin condensation (n) with disappearance of the nucleolus. Notice the dense irregular apical microvilli (mv), absence of basal infolding, numerous vesicular mitochondria (green circles), numerous lysosomes (black circle), cytoplasmic vaculation (v) and thickened cellular BMs (yellow arrow). X٣٦٠٠

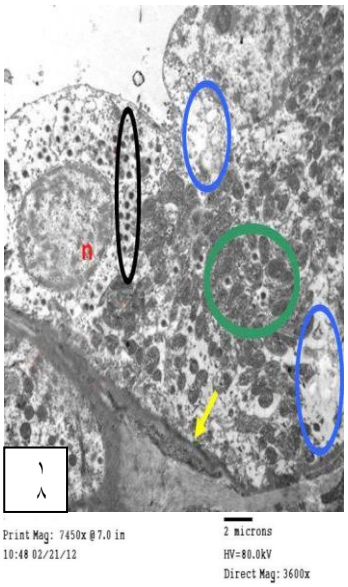

Fig.١٨: An electromicrograph of the DCT cells of group II showing swollen cells with more nuclear chromatin condensation (n), disappeared nucleolus, and basal infolding. Notice numerous swollen mitochondria (green circle), lysosomes (black circle), cytoplasmic vacuolation (blue circles) and more thickening of the cellular BMs (circle). X٣٦٠٠

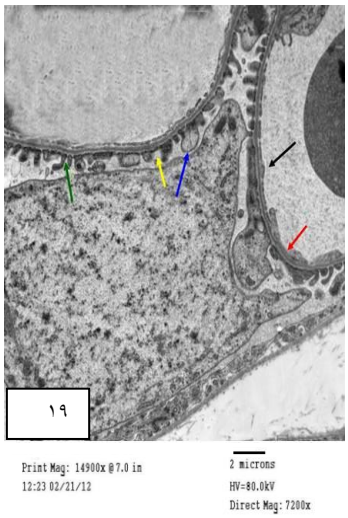

Fig.١٩: An electromicrograph of a renal glomerulus of group III showing blood capillaries with irregular fenestrae (black arrow) and few wide pedicles (blue arrow). Notice the narrow (green arrow) and wide (yellow arrow) filtration slits in the same glomerulus. The glomerular BMs (red arrow) become less thickened compared to group II. X٧٢٠٠

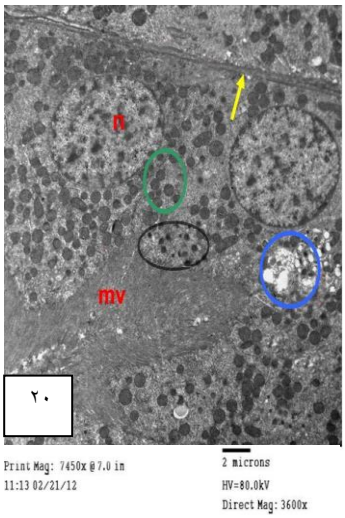

Fig.٢٠: An electromicrograph of the PCT cells of group III showing less nuclear chromatin condensation (n) with disappeared nucleoli, dense irregular apical microvilli (mv), absence of basal infolding. Notice Less vesicular mitochondria (green circle), lysosomes (black circle), cytoplasmic vacuolation (blue circle), and less thickened cellular BMs (circle) compared to group II. X٣٦٠٠

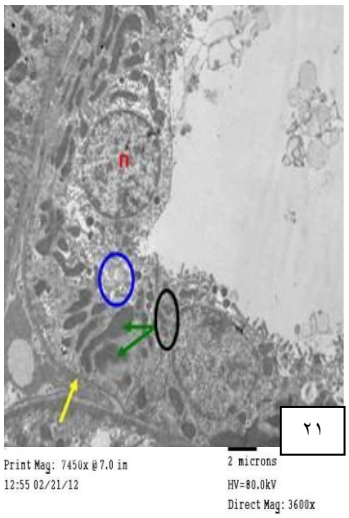

Fig.٢١: An electromicrograph of the DCT cells of group III showing less nuclear chromatin condensation (n) with disappeared nucleoli and basal infolding, less noticeable swollen mitochondria (green arrows), lysosomes (black circle) and cytoplasmic vaculation (blue circle) than in group II. The cells appear shorter and with less thickened BMs (yellow arrow). X٣٦٠٠

Discussion

The results of this study showed an increase in renal function testes; urea and creatinine plasma levels, in the $Cd(Cl)_2$ exposed group; group II, which was in agreement with Ahmed and Abd El- Mottaleb[٢٠] who decided that this increase reflected the progressive impairment of renal clearance of these metabolites which could be referred to parenchyma tissue injury which confirmed by our histological results.

In this work, group III which exposed to $Cd(Cl)_2$ and NSO showed a significant decrease in urea and creatinine levels. This finding was in accordance to Saleem et al.,[٢١] who suggested that, NSO had nephron-prtotective effect as it lowered the values of nephro-toxicity indicators (serum creatinine, blood urea nitrogen, and anti-oxidant activity). Also Ahmed and El-Mottaleb (٢٠) found that concomitant administration of NSO and acetaminophen produced a significant normalization of physiological parameter as Na, and K.

In this study the histological observations showed patchy and variable morphological changes in the renal cortex after $Cd(Cl)_2$ exposure. By the light microscope, these morphological changes were in the form of peri-tubular capillary dilatation, interstitial hemorrhage, swollen renal glomeruli, glomerular and tubular cell cytoplasmic vacu-lation, and interstitial inflammatory cell infiltration which were in agreement with the renal cortical damage reported in previous studies[٢,٥,٦].

Capillary dilatation, congestion and inter-tubular hemorrhages observed in this work were explained by Prozialeck et al.,[٢] who suggested that Cd increased the vascular permeability by affecting the communicating units between endothelia of the venules and capillaries; as a result, edema, hemorrhage, and necrosis occurred.

Enlargement of some vascular glomeruli with decreased or absence of Bowman's spaces were observed. These finding were supported by El-Sharaky et al.,[٢٢] who suggested that Cd disturbed membranes integrity, generates reactive oxygen species and involved cytotoxic and inflammatory mediators in kidney. This was explained by Nolan and Shaikh[٢٣] who found that, the initial effect of Cd administration was on the integrity and permeability of the vascular endothelium, and this led to increase glomerular size, then the necrotic changes occurred secondary to this effect led to shrinkage or contraction of glomeruli.

Regarding the dilated tubules observed in this study, Kukner et al.,[٢٤] suggested that this dilatation might be a compensatory mechanism after the loss of renal excretory function of nephrons by tubular necrosis.

Inflammatory cell infiltration was evident invading the parenchyma of the renal cortex reinforced the recorded result which mentioned that Cd had been regarded as one of the inflammation-related xenobiotics as it induced a complex inflammatory response in several cell types[٢٥].

The glomerular ultra-structural changes found in this study included irregular thickening of the GBM, fusion and flattening of secondary podocyte processes, and loss of normal organi-zation of fenestrae. Thickened GBM was a common finding of many pathologic and experimental conditions[٢٤], which lead to increased permeability of glomerular capillaries resulting in proteinuria. Damage to the GBM itself was attributed to ROS (reactive oxygen species) attacking the GBM and damaging its intricate matrix structure. This may occur by direct oxidation of the GBM components or by adduct formation and dimerization of type IV collagen, leading to distortion of the GBM[٢٦].

Fusion and flattening of foot processes were reported to result from direct injury to the podocyte skeleton after exposure to ROS[٢٧] or may develop secondary to the thickened GBM to compensate for the increased glomerular permeability and proteinuria[٢٨].

In the present study, the tubular morphological changes were in the form of gradual loss of apical microvilli, basal infolding, dense nuclear staining, numerous cytoplasmic vaculation, and thickening of the cellular BMs.

Regarding the PCT, the most remarkable structural change was the loss of integrity and distortion of their brush border which was in agreement with Condron et al.,[٢٩] who stated

that Cd could reduce the surface density of microvillus membrane of convoluted tubules per unit cell volume to ١٩٪ in Cd contaminated rats. Also the partial loss of the basal striations, which probably occurred as a result of damage to the cytoskeleton of PCT cells resulting in decreased activities[٣٠]. The observed irregularity and thickening of the tubular BMs could be a compensatory response to the disrupted brush border of PCTs, along which many substances were absorbed. Similarly, studies dealing with the renal lesions of analgesic nephropathy found increased thickness of tubular and capillary BMs[٣١].

Another abnormality seen in the tubular cells in our results was the numerous lysosomes observed after ٢-wks of $Cd(Cl)_٢$ exposure. Lysosomes when exposed to toxic insults increase in size and number and undergo phospholipidosis[٣٢]. The increase in lysosomes might be an attempt to digest this heavy metal or toxic substance, and this was considered a general manifestation of injury[٣٣].

The mitochondrial swelling observed in this study might reflect the disturbances in oxy-reduction processes taking place in this organelle[٣٤]. Furthermore, it might result from a changed intra-mitochondrial redox potential or an increased mitochondrial production of oxgen free radical[٣٥]. So because the prime source of cell energy in the mitochondria (which were severely damaged), these alterations were sufficient for impairment of other cellular structures and functions[٣٦].

The glomerular and tubular cell cytoplasmic vacuolization observed in this work could by explained by Tripathi and Srivastav[٣٧], who suggested that Cd might cause a failure in the ion pump transport of tubular cells which caused swelling of epithelium and degeneration of tubules. These alterations also suggested incapability of renal cells to cope with functional disturbances provoked by this toxic substance.

Cyclooxygenase (COX) is an enzyme that is responsible for formation of important bio-logical mediators called prostanoids, including prostaglandins, prostacycline and thromboxane. The $COX_٢$ is undetectable in most normal tissue. It is an inducible enzyme in most tissues exposed to inflammation, while in the kidney $COX_٢$ expression exhibits constitutive expression[٣٨]. As inflammation could play a major role in the renal damage produced by exposure to $Cd(Cl)_٢$, one of the purposes of this study was to assess the expression of COX٢ enzymes associated with inflammation.

In this study immune-histochemical detection of $COX_٢$ showed that $COX_٢$ expression was faint and restricted to MDCs in the control group. Komhoff[٣٩] added that $COX_٢$ in rat MDCs was related to renin release. The expression after ٢-wks of $Cd(Cl)_٢$ exposure was higher than in control rats, not only restricted to MDCs but also extend to involve some PCT and DCT cells, which was the same line in other models of renal toxicity and renal failure[٤٠,٤١]. This increased expression could be explained by Figueiredo-Pereira et al.,[٤٢] who found a relationship between oxidative stress induced by Cd exposure in vitro and the induction of COX٢ in a mouse neuronal cell line.

The current study declared that the deleterious effects of $Cd(Cl)_٢$ on the renal structure were noticeably ameliorated by supplementation with NSO. At the light and electron microscope level, this improvement was in the form of less noticeable cytoplasmic vaculation and distortion in glomerular and tubular cells. Hemorrhages, inter-tubular fibrosis and thickening of the BMs (glomerular and tubular) appeared to be remarkably attenuated. NSO administration showed also reduction in the interstitial inflammatory cell infiltration and preservation of the general structural architecture. It was also in accordance to Sultan et al.,[٤٣] who found that, NSO supplementation was more effectual in ameliorating the multiple organ toxicity in oxidative stressed modeling.

The Cd induced nephron-toxicity is thought to be mediated through the accumulation of free radicals as the consequence of increased lipid peroxidation and oxidative deterioration of proteins and DNA [٤٤]. NSO was proved to have strong anti-oxidant properties due to its ability to scavenge free radicals and inhibit lipid peroxidation [٤٥].

Another reason for the protective effect of NSO thought to be related to the improving mitochondrial function, also NSO was reported to produce a marked inhibition of leukotrieens

release, which caused mucosal tissue injury and hypoxemia [٤٦]. Therefore, it might favor cyto-protection.

It was clearly noticed the remarked reduction in the vesicular mitochondria of PCT and DCT cells after ٢-wks of NSO exposure. This finding were supported by the results of Mahmoud et al.,[٣٢] and Alhibshi et al.,[٤٧] who suggested that, Thymoquinone, the main constitute of the volatile oil of NSO, was effective in protecting against nephro-toxicity, possibly via increased mitochondrial function and ATP production.

Conclusion and Recomendations:

It could be concluded that exposure of rats to $Cd(Cl)_٢$ induced Nephron-toxicity while administration of NSO ameliorate this toxic effect.

Our study suggested that a diet rich in natural NSO or used as a herbal medicine could be useful to prevent $Cd(Cl)_٢$ induced nephron-toxicity in humans who are highly exposed to that toxicant (eg. industrial areas or smokers). Further investigations on the mechanism of action of NSO are required and may have a considerable impact on future clinical treatment of patients with acute renal failure. Further studies are also needed to explain Cd - NSO interaction in condition of long term co-exposure and their consequences for health.

Refereences

١. Mustafa T, Srivastava C, and Jensen B. Pharmacology of ginger, zingiber officinale. J drug dev. ١٩٩٣; ٦:٢٥-٣٩.

٢. Prozialeck, Lamar P, and Lynch S. Cadmium alters the localization of N-cadherin, E-cadherin and beta-catenin in the proximal tubule epithelium. Toxicol Appl Pharm. (٢٠٠٦); ١٨٩: ١٨٠–١٩٥.

٣. Satarug S, Ujjin P, Vanavanitkun Y, Nishijo M, Baker J. and Moore M. Effects of cigarette smoking and exposure to cadmium and lead on phenotypic variability of hepatic CYP٢A٦ and renal function biomarkers in men. Toxicology. ٢٠٠٤; ٢٠٤:١٦١–١٧٣.

٤. Jarup L and Akessom A. current status of cadmium as environmental health problem. Toxicology and applied pharmacology. ٢٠٠٩; ٣: ٢٠١-٢٠٨.

٥. Klassen C, Liu J, and Diwan B. Metallothionein protection of cadmium toxicity. Toxicol. Appl. Pharmacol. ٢٠٠٩; ٢٣٨: ٢١٥–٢٢٠.

٦. Liu Y, Liu J, Habeebu S, Waalkes M, and Klaassen C. Metallothionein I/II null mice are sensitive to chronic oral cadmium-induced nephron-toxicity. Toxicol Sci. ٢٠٠٠; ٥٧: ١٦٧–١٧٦.

٧. Nishijo M, Morikawa Y, Nakagawa H, Tawara K, Miura K and Kido T. Causes of death and renal tubular dysfunction in residents exposed to cadmium in the environment. Occup Environ Med. ٢٠٠٥; ٦٣(٨):٥٤٥–٥٥٠.

٨. Majdalawieh F, Hmaidan R and Carr I. Nigella sativa modulates splenocyte proliferation Th١/Th٢ cytokineprofile macrophage function and NK anti-tumor activity. Journal of Ethno. Pharmacology. ٢٠١٠; ١٣١: ٢٦٨-٢٧٥.

٩. Mohamadin M, Sheikh B, Abd El-Aal A, et al. Protective effects of Nigella sativa oil on propoxu-rinduced toxicity and oxidative stress in rat brain region". Pesticide Biochemistry and Physiology. ٢٠١٠; ٩٨:١٢٨-١٣٤s.

١٠. Tariq M. Nigella sativa seeds: folklore treatment in modern day medicine". Saudi J. Gastroenterol. ٢٠٠٨; ١٤: ١٠٥-١٠٦.

١١. Alenzi Q, El-Bolkiny S, and Salem L. Protective effects of Nigella Sativa Oil and thymoquinone against toxicity induced by the anticancer drug cyclopho-sphamide". Br. J. Biomed.Sci. ٢٠١٠; ٦٧: ٢٠-٢٨.

١٢. Mansour M, Nagi M, El-Khatib A; and Al-Bekairi A. Effects of thymoquinone on antioxidant enzyme activities lipid peroxidation and DT-diaphorase in different tissues of mice: a possible mechanism of action. Cell Biochem. Funct. ٢٠٠٢; ٢٠: ١٤٣-١٥١.

١٣. Mansour A, Ginawi T, El-Hadiyah T, El-Khatib S, Al-Shabanah A, and Al-Sawaf A. Effects of volatile oil constituents of Nigella sativa on carbon tetrachloride-induced hepatotoxicity in mice: evidence forantioxidant effects of thymoquinone. Res Commun Mol Pathol Pharmacol. ٢٠٠١; ١١٠: ٢٣٩-٢٥١.

١٤. Kanter M, Demir H, Karakaya C, and Ozbek H. Gastroprotective activity of Nigella sativa oil and its constituent thymoquinone against acute alcohol-

induced gastric mucosal injury in rats. World J. Gastroenterol. ٢٠٠٤; ١١: ٦٦٦٢-٦٦٦٦.

١٥. Young D. Effects of Disease on Clinical Laboratory Tests ٤th edition. ٢٠٠١;٣:٦٧–٦٩

١٦. Bancroft J and Garble M. Theory and Practice of Histological Techniques. ٦th ed. Harcourt: Churchill Livingstone: (٢٠٠٧); ٨٥-٩٨.

١٧. Côté A, Silva R, and Cuello A. Current protocols for light microscopy immunocytochemistry. In: Cuello AC editor. Immunohistochemistry II: John Wiley & Sons Chichester. ١٩٩٣;١٤٧-١٦٨.

١٨. Bozzola J and Russell D. Electron microscopy: Principles and techniques for biologists. ٢nd ed. Jones and Bartlett Publishers.١٩٩٨; ١٦-١٨.

١٩. Houghton D, Plamp C, Defehr J, Bennett W, Forter G, and Gilbert D. Gentamicin and tobramycin nephrotoxicity. Am J Pathol. ١٩٧٨; ٩٨: ١٣٧-١٥٢.

٢٠. Ahmed O, and El- Mottaleb N. Renal function and arterial blood pressue alterations after exposure to acetaminophen with a potential role of Nigella sativa oil in adult male rats. physiol Biochem. ٢٠١٣; ٦٩:١-١٣.

٢١. Saleem U, Reham K, and Eum A. Nephro-protective effect of vitamin c and Nigella sativa oil on gentamicin associated nephrotoxicity in rabbits. Pak j pharm Sci. ٢٠١٢; ٢٥: ٧٢٧-٧٣٠.

٢٢. El-Sharaky S, Newairy A, Badreldeen M, Eweda M, and Sheweita A. Protective role of selenium against renal toxicity induced by cadmium in rats. Toxicology. ٢٠٠٧; ٢٣٥(٣): ١٨٥-١٩٣.

٢٣. Nolan C and Shaikh Z. The vascular endothelium as a target tissue in acute cadmium toxicity. Life Sci.١٩٨٦; ٣٩: ١٤٠٣-١٤٠٩.

٢٤. Kukner A, Colakoglu N, Kara H, Oner H, Ozogul C and Ozan E. Ultrastructural changes in the kidney of rats with acute exposure to cadmium and effects of exogenous metallothionein. Biol. Trace Elem. Res. ٢٠٠٧; ١١٩ ١٣٧–١٤٦.

٢٥. Souza V, Escobar, M, Gomez-Quiroz L, Bucio L, Herna´ndez E, Cossio E, and Gutierrez-Ruiz M. Acute cadmium exposure enhances AP-١ DNA binding and induces cytokines expression and heat shock protein ٧٠ in HepG٢ cells. Toxicology. ٢٠٠٤; ١٩٧: ٢١٣– ٢٢٨.

٢٦. Mostafa M. Effect of cadmium on the renal cortex of adult albino rat and the possible protective role of alpha-lipioc acid. Egypt J Anat. ٢٠١٠; ٣٣:٥٥–٧٠.

٢٧. Riedle B and Kerjaschki D. Reactive oxygen species cause direct damage of Engelbreth-Holm-Swarm matrix. Am J Pathol. ١٩٩٧; ١٥١:٢١٥–٢٣١.

٢٨. Ricardo SD, Bertram JF, Ryan GB. Reactive oxygen species in puromycin aminonucleoside nephrosis: in vitro studies. Kidney Int. ١٩٩٤; ٤٥:١٠٥٧–١٠٦٩.

٢٩. Mohamed SA and El-sharkawy SA. Histological study of early and late nephrotoxicity and endothelial cytotoxicity of ionic and non-ionic contrast media. Egypt J Anat. ١٩٩٥; ١٨:١١٥–١٣٢

٣٠. Condron R, Schroen C, and Marshall A. Morphometric analysis of renal proximal tubules in cadmium-treated rats. J Submicrosc Cyto Pathol. ١٩٩٤; ٢٦: ٥١-٥٨.

٣١. Eknoyan G. Analgesic nephrotoxicity and renal papillary necrosis. Semin Nephrol. ١٩٨٤; ٤:٦٥–٧٦.

٣٢. Mahmoud FY and El-Badry M. Histological effects of gentamicin intake during pregnancy on the liver and kidney of the fetus and mother of albino rat. Egypt J Anat. ٢٠٠١; ٢٤:٣٥–٥٧.

٣٣. Joles JA, Kunter U, Janssen U, Kriz W, Rabelink TJ, Koomans HA, Floege J. Early mechanisms of renal injury in hypercholesterolemic or hypertriglyceridemic rats. J Am Soc Nephrol. ٢٠٠٠; ١١:٦٦٩–٦٨٣.

٣٤. Thevenod F. Nephrotoxiciry and the proximal tubule. Insights from cadmium. Nephron Physiol. ١٩٩٨; ٩٣: ٨٧-٩٣.

٣٥. Yang X, Borg C, and Siman M. Maternal antioxidant treatments prevent diabetes-induced alterations of mitochondrial morphology in rat embryos Anat. Rec. ١٩٩٨; ٢٥١: ٣٠٣–٣١٥

٣٦. Asar M, Kayisli A, and Izgut N. Cadmium-induced changes in parietal cell structure and functions of rats. Biol. Trace Element Res. ٢٠٠٠; ٧٤: ١٥٣–١٧٠.

٣٧. Tripathi S and Srivastav A. Cytoarchitectural alterations in kidney of Wistar rat after oral exposure to cadmium chloride. Tissue and cell. ٢٠١١; ٤٣:١٣١-١٣٦.

٣٨. Warner T and Mitchell J. Cyclooxygenase-٣ (COX-٣): filling in the gaps toward a

COX continuum. Proc Natl Acad Sci USA. ٢٠٠٢; ٩٩: ١٣٣٧١-١٣٣٧٣.

٣٩. Komhoff M. Cyclooxygenase-٢-selective inhibitors impair glomerulogenesis and renal cortical development. Kidney Int. ٢٠٠٠; ٥٧: ٤١٤-٤٢٢.

٤٠. Salgado C, Barbero A, Eleno N, and Lo´pez-Novoa J. Gentamicin induces Jun-AP١ expression and JNK activation in renal glomeruli and cultured mesangial cells. Life Sci. ٢٠٠٥; ٧٧: ٢٢٨٥–٢٢٩٨.

٤١. Morales A, Vicente C, Jerkic M, Jose M, Santiago B, Novoa L. Effect of quercetin on metallothionein nitric oxide synthases and cyclooxygenase-٢ expression on experimental chronic cadmium nephron-toxicity in rats. Toxicology and Applied Pharmacology. ٢٠٠٥; ٢١٠: ١٢٨ – ١٣٥.

٤٢. Figueiredo-Pereira M, Li Z, Jansen M and Rockwell P. N-acetylcysteine and celec-oxib lessen cadmium cytotoxicity which is associated with cyclooxygenase-٢ up-regulation in mouse neuronal cells. J. Biol. Chem. ٢٠٠٢; ٢٧٧: ٢٥٢٨٣–٢٥٢٨٩.

٤٣. Sultan M, Butt M, Ahmadm R, Pashal I, Ahmad A, and Qayyum M. Supplemen-tation of Nigella sativa fixed and essential oil mediates potassium bromate induced oxidative stress and multiple organ toxicity. J Pharm sci. ٢٠١٢; ١٧٥-١٨١.

٤٤. Renugadevi J and Prabu S. Naringenin protects against cadmium-induced renal dysfunction in rats. Toxicology. ٢٠٠٩; ٢٥٦ (١-٢): ١٢٨–١٣٤.

٤٥. Ismail M, Al-Naqeep G, Chan W. Nigella sativa thymoquinone-rich fraction greatly improves plasma antioxidant capacity and expression of antioxidant genes in hypercholesterolemic rats. Free Radic Biol Med. ٢٠١٠; ٤٨:٦٦٤–٦٧٢.

٤٦. Nagi MN, Almakki HA, Sayed-Ahmed MM, Al-Bekairi AM. Thymoquinone supplementation reverses acetaminophen-induced oxidative stress nitric oxide production and energy decline in mice liver. Food Chem Toxicol. ٢٠١٠; ٤٨:٢٣٦١–٢٣٦٥.

٤٧. Alhibshi H, Gotoh I, and Suzuki I. Thymoquinone protect cultured rat primary neurons against amyloid β-induced neurotoxicity. Biochem Biophys Res Commun. ٢٠١٣; ١٩(٤):٣٦٢-٧.